
# Combining Antenna and Ground Plane Tuning to Efficiently Cover Tv White Spaces on Handsets

Barrio, Samantha Caporal Del; Hejselbæk, Johannes; Morris, Art; Pedersen, Gert F.

*Published in:*
2017 11th European Conference on Antennas and Propagation (EuCAP)

*DOI (link to publication from Publisher):*
10.23919/eucap.2017.7928202

*Publication date:*
2017

*Document Version*
Accepted author manuscript, peer reviewed version

# Combining Antenna and Ground Plane Tuning to Efficiently Cover Tv White Spaces on Handsets

Samantha Caporal del Barrio*†, Johannes Hejselbæk*, Art Morris†, Gert F. Pedersen*,
*Section of Antennas, Propagation and Radio Networking (APNet), Department of Electronic Systems,
Faculty of Engineering and Science, Aalborg University, DK-9220, Aalborg, Denmark, scdb@es.aau.dk
†WiSpry Inc., Irvine, CA, USA

***Abstract*—With the future LTE auction for TV white spaces at 600 MHz, there is a strong need for efficient handset antennas operating at very low frequencies. This paper proposes a tunable antenna design for the low bands of LTE. In this design, not only the antenna is tuned but also the resonance of the board, thanks to using a tunable parasitic. The resulting dual-resonant antenna exhibits a peak total efficiency of -4 dB at 600 MHz.**

***Index Terms*—4G mobile communication, Antenna measurements, Reconfigurable architectures, Mobile antennas, Multi-frequency antennas, LTE communications systems, Eigenvalues and eigenfunctions, Impedance loading, Microelectromechanical devices.**

## I. Introduction

The bandwidth specifications for the $4^{th}$ Generation (4G) of mobile communications include bands ranging from 699 MHz to 2.690 GHz. The transition to digital television (TV) freed bands between 600 MHz and 700 MHz, which are being auctioned for LTE. Though low bands offer major advantages in terms of building penetration and coverage, they bring challenges to handset antenna designers given the well-known trade-off between size, bandwidth and efficiency [1]. In order to cover the 600 MHz bands with a handset antenna, frequency-reconfigurability is key. The proposed design uses Micro-Electro-Mechanical Systems (MEMS) tunable capacitors for aperture tuning of the antenna. They are chosen because of their low insertion loss, high voltage handling, and very low power consumption [2]. Related work with MEMS capacitors includes [3], [4].

Frequency-tuning enhances the total antenna bandwidth. However, when the antenna is forced into resonance at a lower frequency than its natural frequency, its Q increases. This affects the currents on the antenna structure and can have a dramatic effect on the total efficiency due to the Equivalent Series Resistance (ESR) loss of the tuning component. It has been shown that loading the ground plane enables to lower its resonance frequency [5]–[9]. Moreover, decreasing the resonance frequency of the ground plane as the antenna is tuned down lowers the Q, thus leads to lower surface currents and to lower power dissipation. As a result, the radiation efficiency is enhanced. This paper is an extension of the work in [10] and shows the measured antenna performance with two very high-Q MEMS tunable capacitors on the design, as opposed to only one shared tuner. This paper shows the implementation, the measured performance and the band coverage of the dual-band design with two separate 1041 tuners, i.e. one on the antenna feeding line and one on the tunable ground.

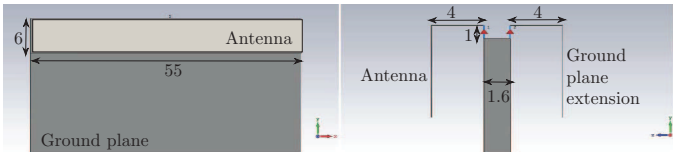


Fig. 1: Antenna geometry in front view (left) and side view (right). Dimensions are given in mm.

Firstly the antenna design is presented in II. Then, the measurements are detailed in III and show the return loss, the total efficiency in the low bands of LTE and the band coverage. Finally, conclusions are drawn in IV.

## II. Tunable design

### A. Tunable antenna

In the proposed design, simultaneous tuning of the antenna operating frequency and of the ground plane resonance frequency is performed. Fig. 1 shows the geometry of the proposed design. A 55 mm $\times$ 6 mm $\times$ 4 mm antenna is used on a 120 mm $\times$ 55 mm Printed Circuit Board (PCB). It is made tunable with a tunable LC circuit on the feeding line. The dimensions of the antenna are identical to the ones of the Ground Plane Extension (GPE), which is connected through a tunable LC circuit to the board. There is no connection between the antenna and the GPE, as between the feeding line and the GPE. While the geometry of the antenna is identical to the one used in [10], the tuning circuitry is different and it is depicted in Fig. 2. In addition to the two 1041 MEMS tunable capacitor packages, the circuitry includes high-Q air inductors (L1 and L2) from Coilcraft [11] and a 0402 fixed capacitor ($C_m$) from Murata [12].

### B. Tunable network

In the previous work [10], a shared 1040 tuner was tested. This work uses two 1041 tuners: a single 1041 tuner on the antenna feeding network and another 1041 tuner for the GPE tuning. The 1040 and the 1041 tuners differ mainly by their Q and capacitance range. In fact, the maximum capacitance of the 1040 tuner is the double than that of the 1041 tuner but its Q is 1.4 times lower. The values of the matching components L1, L2 and $C_m$ are different to fit each tuner,

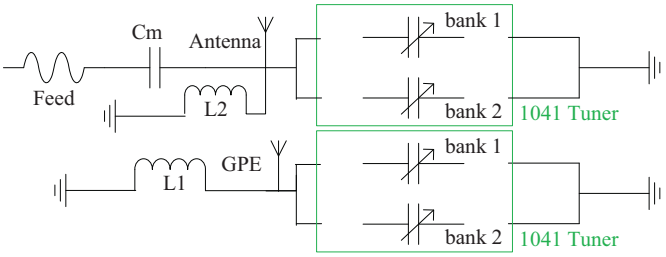


Fig. 2: Tuning schematics, where $C_m$=2.2 pF, L1=5.4 nH and L2=3.8 nH. The 1041 tuners are MEMS tunable capacitors from wiSpry [13].

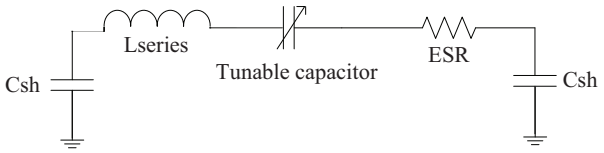


Fig. 3: Schematic of one bank of a MEMS tunable capacitor from wiSpry [13].

which yields different ESR values. The frequencies are also different because of the new tuning range. Therefore, even though the 1041 tuner exhibits a higher Q, the conclusion on antenna efficiency is not straightforward.

The MEMS package comprises a series inductance and a shunt capacitance, i.e. parasitics. They are mainly responsible for the minimum capacitance of the tuner. The 1041 packaged MEMS tuners from wiSpry [13] has a series inductance $L_{series}$ of 4.5 $\times$ $10^{-4}$ nH and a shunt capacitance $C_{sh}$ of 1 pF, throughout the operating frequency range. The simplified schematic of one bank of the MEMS tuner is shown in Fig. 3. The characteristics of the MEMS tunable capacitors are summarized in Table I. The $C_{max}$ value is given for the whole chip, i.e. both banks at maximum capacitance. However, the Q and the ESR are given at the relevant amount of capacitance, i.e. 5.9 pF. In the case of the 1040 design (one shared tuner case), this amount of capacitance corresponds to half of the maximum capacitance of the chip. In the case of the 1041 design (two separate 1041 tuners), it corresponds to the maximum capacitance of the chip. Nevertheless, in both cases, it corresponds to the amount of capacitance needed to tune the antenna to 600 MHz. It is worth noting that, with a fixed capacitor, the Q increases as the frequency decreases. In the case of a tunable capacitor, the Q has to take into account the varying capacitance as well. That is, at the highest antenna operating frequency the tuner is set to its minimum capacitance, and at the lowest antenna operating frequency the tuner is set to its maximum capacitance. Therefore, with respect to frequency and capacitance settings, both the Q and the ESR decrease as we operate on lower bands. The specific Q and ESR values at 850 MHz (cellular bands in USA) and 600 MHz (TV space available for LTE) are summarized in Table I.

TABLE I: Characteristics of the MEMS tunable capacitors

| Characteristics | 1040 | 1041 |
|---|---|---|
| $C_{min}$ [pF] | 0.5 | 0.3 |
| $C_{max}$ [pF] | 11.9 | 6.6 |
| $C_{step}$ [pF] | 0.125 | 0.062 |
| Q at 850 MHz at $C_{min}$ | 691 | 516 |
| ESR at 850 MHz at $C_{min}$ [Ω] | 0.5 | 0.9 |
| Q at 600 MHz at C=5.9 pF | 164 | 227 |
| ESR at 600 MHz at C=5.9 pF [Ω] | 0.3 | 0.2 |

## III. Measurements

### A. Prototype

Pictures of the final demonstrating boards are shown in Fig. 4. The tuning network is hidden by the antenna. On the back side, there is only the GPE. C1-C4 and C6-C9 are DC supply control capacitors and are not involved with RF lines. Fig. 4 (a) shows the entire 120 mm $\times$ 55 mm board and Fig. 5 shows a view from the top. Each element has a height of 4 mm and the PCB has a thickness of 1.6 mm. In order to show the difference of the implementation proposed in this paper, Fig. 4 (b) focuses on the tuning and matching components used for the 1040 design in [10] whereas Fig. 4 (c) focuses on the tuning and matching components used for the proposed design, where two independent 1041 tuners are used. One tuner is used for the antenna only, and another one is used for the GPE only, as could be seen in the schematics in Fig. 2.

### B. Results

The advantage of using the 1041 tuners is their higher Q. The characteristics of the tuner are summarized in Table I. One of the tuners (the tuner 1) is connected to the antenna, while the second tuner (tuner 2) is connected to the GPE, as summarized in Fig. 2. The settings of the tuners used on the antenna and the GPE are summarized in Table II. The matching components and their respective ESR are detailed in Table III. The return loss of the demonstrator is shown in Fig. 6. The measured total efficiency is shown in Fig. 7. The peak total efficiencies are measured to be -1.4 dB at 808 MHz, -2.2 dB at 735 MHz, -3 dB at 692 MHz and -4.2 dB at 630 MHz. The mismatch loss is negligible at resonance. The loss decomposition at 630 MHz is calculated from the simulations and the results are summarized in Table IV. The loss of the tuner is negligible, mainly because its Q is very high and because its two banks are connected in parallel.

### C. Band coverage

The LTE and LTE-A bands are defined by the 3rd Generation Partnership Project (3GPP) in the technical report [14]. In the proposed demonstrator, state 4 and 5 address frequencies below 699 MHz. These frequencies are part of the television white spaces, but below the lowest frequency defined in 3GPP

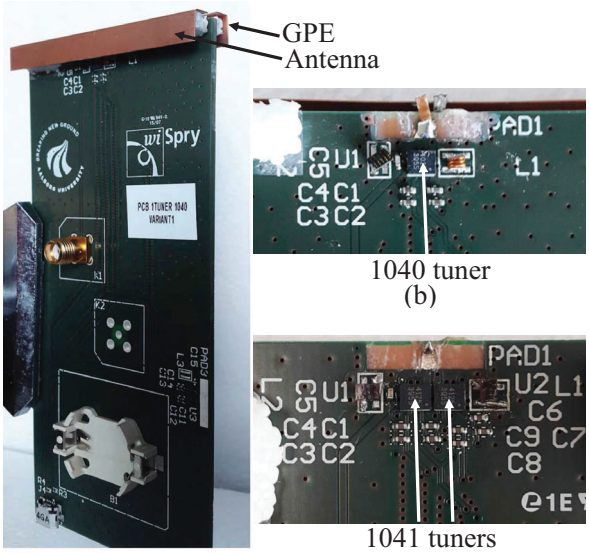


Fig. 4: Demonstrator boards. (a) Demonstrator with the antenna and the GPE mounted. (b) Detailed view of the matching and tuning network for the 1040 design in [10]. The MEMS tuner (U1) has two independent banks, one for controlling the antenna and one for controlling the GPE. (c) Detailed view of the matching and tuning network for the proposed design with two 1041 tuners: U1 and U2. U1 controls the antenna and is connected to C5 and L2. U2 controls the GPE and is connected to L1.

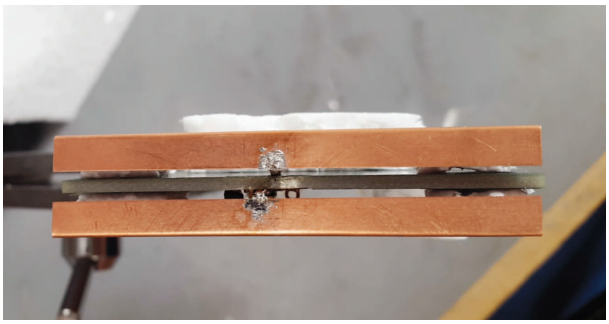

Fig. 5: View of the antenna and the GPE from the top.

TABLE II: MEMS tuner settings for design B

| States | tuner 1 [pF] | tuner 2 [pF] |
|---|---|---|
| State 1 | 0.00 | 0.00 |
| State 2 | 2.25 | 0.6 |
| State 3 | 3.75 | 1.45 |
| State 4 | 4.90 | 2.45 |
| State 5 | 5.90 | 3.95 |

TABLE III: ESR of fixed components in the proposed design

| Fixed component | ESR at 850 MHz [Ω] | ESR at 600 MHz [Ω] |
|---|---|---|
| $C_m$ = 2.2 pF | 0.12 | 0.13 |
| L2 = 3.9 nH | 0.17 | 0.14 |
| L1 = 5.4 nH | 0.21 | 0.18 |

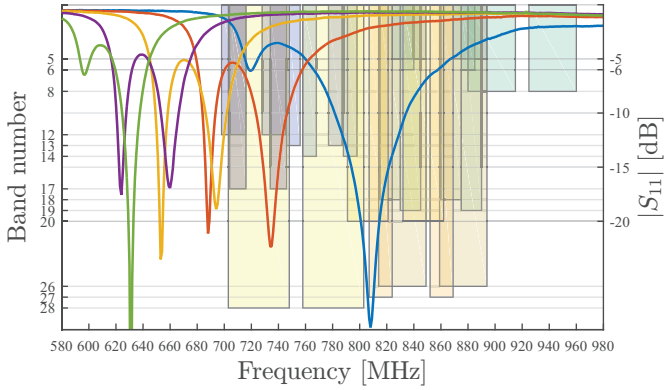


Fig. 6: Return loss of the proposed tunable design when the MEMS tuner varies according to Table II, where the blue curve corresponds to the lowest capacitance setting (state 1) and the green curve corresponds to the highest capacitance setting (state 5) of the tuner.

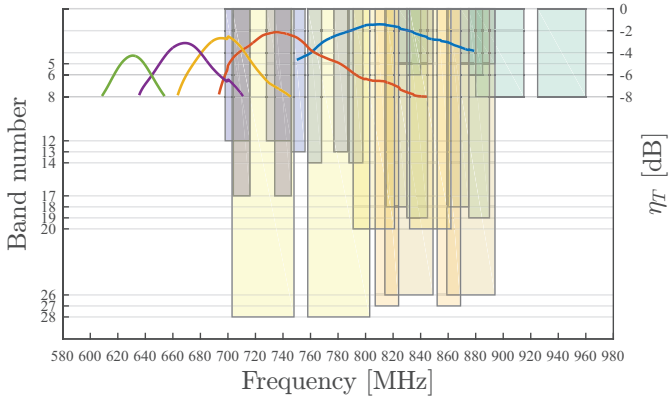


Fig. 7: Total efficiency of the proposed tunable design when the MEMS tuner varies according to Table II, where the blue curve corresponds to the lowest capacitance setting (state 1) and the green curve corresponds to the highest capacitance setting (state 5) of the tuner.

TABLE IV: Loss decomposition of proposed tunable design

| | Loss at 630 MHz [dB] |
|---|---|
| Copper + trace + Fr-4 | 2.5 |
| $C_m$ = 2.2 pF | <<0.1 |
| L2 = 3.9 nH | 0.6 |
| L1 = 5.4 nH | 0.7 |
| 1041 tuner 1 | <<0.1 |
| 1041 tuner 2 | <<0.1 |
| Total radiation | 3.8 |
| Mismatch | 0.4 |
| Total | 4.2 |

TABLE V: Return loss bandwidths at -6 dB

| State | Impedance bandwidth [MHz] |
|---|---|
| 1 | [766-857] |
| 2 | [677-700],[713-758] |
| 3 | [647-664],[677-709] |
| 4 | [618-632],[647-673] |
| 5 | [618-643] |

so far. The Frequency Division Duplex (FDD) bands have been summarized in the return loss (Fig. 6) and total efficiency (Fig. 7) figures for convenience of the reader. Each figure depicts the uplink channels (TX) and the downlink channels (RX), such that the reader can see two blocks for each band. For example, band 8 transmits from 880 MHz to 915 MHz (TX 8) and receives from 925 MHz to 960 MHz (RX 8). The impedance bandwidth, typically read on the return loss figure (Fig. 6), is summarized in Table V.

However, when considering a design that comprises lossy components the efficiency bandwidth is a more informative measure [15]. The efficiency bandwidth can be read on the total efficiency plot, i.e. Fig. 7. The authors chose a threshold at -4 dB for the low bands of LTE. For the proposed dual-band design, the efficiency bandwidths are summarized in Table VI. The efficiency bandwidth for state 5 cannot be calculated for a threshold at -4 dB since the total efficiency peaks at -4 dB. Another way to evaluate the antenna is to look at the low bound on the total efficiency for a given bandwidth around the resonance frequency, as summarized in Table VII for a bandwidth of 40 MHz. It is clear that 40 MHz bandwidth in the 600 MHz bands will greatly affect the low bound on efficiency and that the decisions on channel bandwidths and duplex spacing must take these parameters into account, in order to efficiently address such low frequencies with electrically small antennas. To sum up, the following LTE bands can be covered by the proposed dual-band design with an efficiency higher or equal to -4 dB. State 1 covers the bands 5, 6, 18, 13, 14, 20

TABLE VI: Efficiency bandwidths at -4 dB

| State | Frequency interval | Bandwidth [MHz] |
|---|---|---|
| 1 | [880-759] | 121 |
| 2 | [763-707] | 56 |
| 3 | [712-680] | 32 |
| 4 | [680-656] | 24 |
| 5 | - | - |

TABLE VII: Efficiency low bound for 40 MHz bandwidth

| State | Frequency interval | Lowest efficiency [dB] |
|---|---|---|
| 1 | [830-790] | -1.9 |
| 2 | [755-715] | -3.2 |
| 3 | [713-673] | -4.4 |
| 4 | [688-648] | -5.3 |
| 5 | [651-611] | -7.4 |

and 27. State 2 covers the bands 12 and 17. Below 699 MHz, the channel bandwidths have not been specified yet, nor are the duplex spacings.

## IV. Conclusion

This paper presents a tunable antenna design, where the antenna and the ground plane are tuned simultaneously with two different MEMS tunable capacitors. Measurements yield a peak total efficiency of -3 dB at 700 MHz and -4 dB at 600 MHz. Though the GPE adds volume, the design does not require a cut-back on the PCB, which is a real advantage to manufacturers. Future work concerns MIMO capabilities of the proposed design.

## References


[1] R. F. Harrington, "Effect of Antenna Size on Gain, Bandwidth, and Efficiency," *Journal of Research of the National Bureau of Standards - Radio Propagation*, vol. 64D, no. 1, pp. 1–12, 1960.

[2] N. Haider, D. Caratelli, and a. G. Yarovoy, "Recent Developments in Reconfigurable and Multiband Antenna Technology," *International Journal of Antennas and Propagation*, vol. 2013, pp. 1–14, 2013.

[3] Q. Gu and J. R. D. Luis, "RF MEMS Tunable Capacitor Applications in Mobile Phones," in *Solid-State and Integrated Circuit Technology (ICSICT), 2010 10th IEEE International Conference on*, pp. 1–4, 2010.

[4] J. Ilvonen, R. Valkonen, J. Holopainen, and V. Viikari, "Multiband Frequency Reconfigurable 4G Handset Antenna with MIMO Capability," *Progress In Electromagnetics Research (PIER)*, vol. 148, no. August, pp. 233–243, 2014.

[5] S. Wang and Z. Du, "A Dual-Antenna System for LTE/WWAN/WLAN/WiMAX Smartphone Applications," *Antennas and Wireless Propagation Letters*, vol. 14, pp. 1443–1446, 2015.

[6] F.-H. Chu and K.-L. Wong, "Planar Printed Strip Monopole-With a Closely-Coupled Parasitic Shorted Strip for Eight-Band LTE/GSM/UMTS Mobile Phone," *IEEE Transactions on Antennas and Propagation*, vol. 58, no. 10, pp. 3426–3431, 2010.

[7] C.-h. Chang and K.-l. Wong, "Bandwidth Enhancement of Internal WWAN Antenna Using an Inductively Coupled Plate in the Small-size Mobile Phone," *Microwave and Optical Technology Letters*, vol. 52, no. 6, pp. 1247–1253, 2010.

[8] A. Cihangir, F. Ferrero, C. Luxey, G. Jacquemod, and P. Brachat, "A Bandwidth-Enhanced Antenna in LDS Technology for LTE700 and GSM850 / 900 Standards," in *European Conference on Antennas and Propagation (EUCAP)*, no. Eucap, pp. 2706–2709, 2013.
[9] Y.-l. Ban, C.-l. Liu, J. L.-w. Li, and R. Li, "Small-SizeWideband Monopole With Distributed Inductive Strip for Seven-Band WWAN/LTE Mobile Phone," *IEEE Antennas and Wireless Propagation Letters*, vol. 12, pp. 7–10, 2013.
[10] S. Caporal del Barrio, E. Foroozanfard, G. F. Pedersen, and A. Morris, "Tunable Handset Antenna: Enhancing Efficiency on TV White Spaces," *IEEE Transactions on Antennas and Propagation*, vol. pre-pub, 2016.
[11] Coilcraft and A. C. Inductors, "http://www.coilcraft.com/sq_spring.cfm."
[12] Http://www.murata.com/products/catalog/pdf/c02e.pdf, "Murata Chip Monolithic Ceramic Capacitors," 2012.
[13] WiSpry, "http://www.wispry.com/products-capacitors.php," 2014.
[14] TR136.912 - V12.0.0 - Rel12, "LTE; Feasibility study for Further Advancements for E-UTRA (LTE-Advanced)," tech. rep., 3GPP, 2014.
[15] J. Rahola and R. Valkonen, "Using the concept of obtainable efficiency bandwidth to study tunable matching circuits," *Proceedings of 6th European Conference on Antennas and Propagation, EuCAP 2012*, pp. 1869–1872, 2012.